

# Artificial Intelligence in Brain Tumor Imaging

Subjects: Oncology

Contributor: Maurizio Cè, Giovanni Irmici, Chiara Foschini, Giulia Maria Danesini, Lydia Viviana Falsitta, Maria Lina Serio, Andrea Fontana, Carlo Martinenghi, Giancarlo Oliva, Michaela Cellina

The application of artificial intelligence (AI) is accelerating the paradigm shift towards patient-tailored brain tumor management, achieving optimal onco-functional balance for each individual. AI-based models can positively impact different stages of the diagnostic and therapeutic process. Although the histological investigation will remain difficult to replace, in the near future the radiomic approach will allow a complementary, repeatable and non-invasive characterization of the lesion, assisting oncologists and neurosurgeons in selecting the best therapeutic option and the correct molecular target in chemotherapy. AI-driven tools are already playing an important role in surgical planning, delimiting the extent of the lesion (segmentation) and its relationships with the brain structures, thus allowing precision brain surgery as radical as reasonably acceptable to preserve the quality of life. AI-assisted models allow the prediction of complications, recurrences and therapeutic response, suggesting the most appropriate follow-up.

Keywords: artificial intelligence ; brain tumors ; glioblastoma ; deep learning ; prognosis prediction

---

## 1. Introduction

Even though artificial intelligence (AI) is far from being used routinely in the current workflow of radiologists, the number of clinical studies using radiomics and radiogenomics approaches in neuroradiology is increasing day by day. Here, the researchers describe some examples of AI applications in the main activities related to brain tumor imaging, with a special focus on gliomas. These applications include lesion detection, differential diagnosis, non-invasive molecular characterization, the definition of lesion boundaries and spatial relationships (segmentation), and an assessment of response to therapy and prognosis. It is likely that in each of these areas, AI models will soon play a central role in assisting the radiologist in his daily work <sup>[1]</sup>.

Gliomas are the most common type of central nervous system (CNS) neoplasm and arise from glial cells <sup>[2]</sup>. They represent a clinically and biologically heterogeneous disease, with several recognized histotypes and molecular subtypes, and a clinical history ranging from slow growth and predominantly benign prognosis, such as pilocytic astrocytoma, to particularly aggressive histological subtypes, such as glioblastoma multiforme (GBM), which is associated with rapid progression and poor prognosis <sup>[3][4]</sup>. Therefore, timely and accurate diagnosis is essential to ensure adequate patient treatment and longtime survival.

Historically, brain tumor classification has been solely based on histopathological features <sup>[5]</sup>, whereas the latest editions incorporate genetic and epigenetic information, such as molecular markers (e.g., IDH mutation, 1p/19q codeletion, etc.) and DNA methylation profiles <sup>[6][7]</sup>. The genetic and epigenetic makeups define the molecular signature, a “barcode” of the tumor, whose recognition is essential for clinical decision-making in the era of targeted therapies <sup>[8]</sup>. Therefore, tissue sampling remains the gold standard for decoding the molecular landscape of most CNS tumors, especially for gliomas <sup>[9]</sup>. Nevertheless, growing evidence has highlighted the powerful role of artificial intelligence in oncological neuroimaging through the extraction of quantitative information from routine radiological examinations <sup>[10]</sup>. Alongside the molecular signature is the imaging signature, which offers complementary and ideally additional information for the characterization of the brain tumor, with a potential role in guiding the choice of the most appropriate therapy and clinical management <sup>[11]</sup>. In this landscape, AI-assisted tools represent the bridge from precision diagnostics to precision therapeutics <sup>[12]</sup>.

In **Figure 1**, the flowchart shows the possible applications of AI in brain tumor imaging to provide customized patient management.

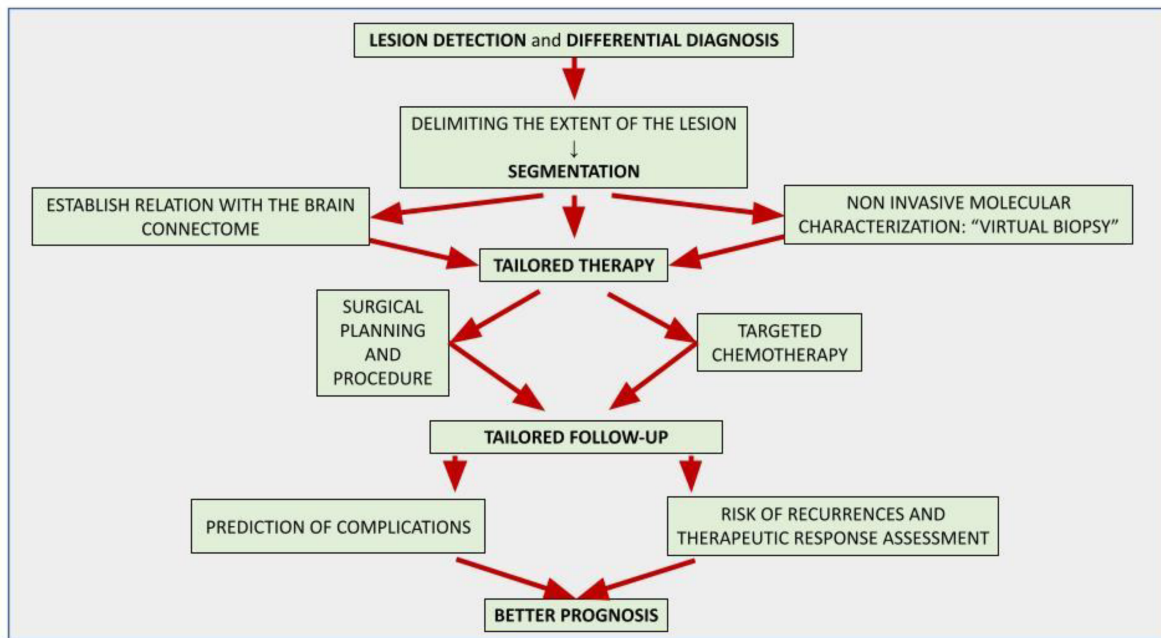


**Figure 1.** The flowchart in Figure 1 represents the developed AI tools for brain tumor imaging and their aim. The final purpose is to provide customized therapy and follow-up for each patient in order to achieve a good outcome.

## 2. An Introduction to Artificial Intelligence and Related Concepts

### 2.1. Artificial Intelligence (AI)

AI can be defined as technology that mimics human cognitive processes, such as learning, reasoning, and problem-solving. Developed as a branch of computer science, present-day AI is a broad field of knowledge that welcomes contributions from different disciplines, such as statistics, informatics, and physics.

### 2.2. Radiomics

Radiomics was first described by Lambin in 2012 as the high-throughput extraction of numerous quantitative image features from radiographic images for diagnostic purposes <sup>[13]</sup>. At the basis of this new approach is the awareness that radiological images must be considered as numerical data rather than simple images, providing much more information than can be perceived by the radiologist through a qualitative evaluation <sup>[14][15][16]</sup>. The radiomic paradigm seeks to extract quantitative and ideally repeatable information from diagnostic images, including complex patterns that are challenging for the human eye to detect or quantify. There are high expectations that the contribution of artificial intelligence to biomedical imaging will help close the gap towards personalized medicine <sup>[17][18]</sup>.

## 3. Lesion Detection and Differential Diagnosis

AI-powered tools can aid neuroradiologists in lesion detection and differential diagnosis.

Since gliomas are often diagnosed when they are large and symptomatic, the detection of glioma-like lesions on MRI may seem relatively trivial to an experienced neuroradiologist. Conversely, the early diagnosis of small brain metastases (BM) in oncological patients during follow-up is challenging, because sensitivity on MRI is variable, and many details of MRI acquisition can impact the performance <sup>[19]</sup>. However, since stereotactic radiosurgery protocols and other therapeutic decisions are based on the number and location of even small metastases, early diagnosis is a real concern for neuroradiologists, given the high impact on the patient's prognosis. For this reason, most of the computer-aided detection (CAD) tools available in the field of neuro-oncology focus primarily on the automated detection of brain metastases.

The proper tuning of CAD tools is essential to ensure diagnostic accuracy, lowering the risk of overdiagnosis, overtreatment, and unreasonable concern in patients <sup>[20]</sup>. Generally speaking, if the threshold sensibility is too low, the model can be affected by a high false-positive rate, for example, including vascular structures instead of small metastases; on the other hand, when the threshold is high, the model can fail to detect small (in particular, <3 mm) lesions <sup>[21]</sup>.

Park et al. have recently demonstrated how DL-based models significantly increase the diagnostic accuracy in the detection of small lesions by exploiting the integration of large amounts of MRI data: in particular, a DL model that combines 3D Black Blood and 3D GRE MRI sequences outperformed a DL model using only 3D GRE sequences in the detection of brain metastases ( $p < 0.001$ ), yielding a sensitivity of 93.1% versus 76.8% [22].

Solitary BM and GBM can exhibit quite similar MRI features, such as post-contrast ring enhancement, necrotic core, and large peritumoral edema presenting with high signal on T2-weighted and FLAIR images [23]. Differentiating these two entities is essential, considering they are the most common brain tumors in the adult population and have quite different treatments [23]. Thus, several researchers have focused on this topic, showing the advantages of multiparametric MRI [24] [25] and, more recently, evaluating the performances of different AI-based classifiers compared to expert neuroradiologists.

For example, Swinburne et al. investigated whether an ML algorithm including advanced MRI (advMRI) data from 26 patients can reliably differentiate between GBMs ( $n = 9$ ), BM ( $n = 9$ ), and primary central nervous system lymphoma (PCNSL) ( $n = 8$ ). Their multilayer perceptron model performed well in discriminating between the three pathological classes. After adopting a leave-one-out cross-validation strategy, the model achieved a maximum accuracy of 69.2%, intermediate to that of two human readers (65.4% and 80.8%). However, the use of the same model for cases where human reviewers disagreed on the diagnosis yielded an increase of 19.2% incorrect diagnoses. No evaluation with an independent test cohort was carried out in this study, and this represents the main limitation of this study [26].

Since the contrast enhancement and local infiltration of white matter bundles are key features of high grade-gliomas (HGGs) [27], most ML and DL algorithms exploit radiomic features extracted on post-contrast T1-weighted 3D images or diffusion-weighted images (DWI) and related techniques, such as diffusion tensor imaging (DTI).

For example, a recent study based on DTI metrics, especially fractional anisotropy (FA) and ADC values, demonstrated that peritumoral alteration is different in these two entities, with GBM showing greater heterogeneity due to the infiltrative nature and aggressive tumor [1][28]

The combination of radiomic and non-radiomic features (clinical and qualitative imaging) has in some cases been shown to be better than using radiomic features alone. For example, a study by Han et al., established the importance of adding clinically relevant data (e.g., age and sex) and routine radiological indices (tumor size, edema ratio, and location) to build an AI-driven model to differentiate between GBM and BM from lungs and other sites using a logistic regression model; the integrated model was superior to the single model [29].

BM can be the first manifestation of a still unknown extracerebral malignancy; therefore, ML tools have been applied in the clinical scenario in which patients are found with brain metastases without a known primary site of cancer [30]. Metastases coming from different primary cancers show differences in the local environments and consequently exhibit different radiomic features [12]. Ortiz-Ramón et al. provided good results in differentiating metastases from lung cancers, melanoma, and breast cancers when they implemented an AI-driven model with two- and three-dimensional texture analyses of T1-weighted post-contrast sequences within a nested cross-validation structure after quantizing the images with multiple numbers of gray-levels to evaluate the influence of quantization [31].

Another challenging differential diagnosis is between GBM and PCNSL since these entities may show similar appearances on conventional MRI, especially when GBMs do not present a necrotic core and the enhancement is not confined to the peripheral area but is more homogeneous [32][33]. Generally, PCNSLs are treated with whole-brain chemotherapy and radiotherapy, while GBM commonly undergoes surgical resection before chemo-radiotherapy [34]; therefore, a proper diagnosis is mandatory.

A recent study by Stadlbauer et al. [35] analyzed the effectiveness of a multiclass ML algorithm that integrates several radiomic features extracted from advanced MRI (including axial diffusion-weighted imaging sequences and a gradient echo dynamic susceptibility contrast (GE-DSC) perfusion) and physiological MRI (protocol including the vascular architecture mapping (VAM) and the quantitative blood-oxygenation-level-dependent (qBOLD)) to classify the most common brain enhancing-tumors: (GBM, anaplastic glioma, meningioma, PCNSL, or brain metastasis). When compared to the human reader, the AI-driven algorithms achieved a better performance, resulting in superior accuracy (0.875 vs. 0.850), precision (0.862 vs. 0.798), F-score (0.774 vs. 0.740), and AUROC (0.886 vs. 0.813); however, the radiologists demonstrated higher sensitivity (0.767 vs. 0.750) and specificity (0.925 vs. 0.902).

The DL paradigm has evolved in recent years as a big data grinding machine and has replaced many conventional algorithms in the field of image analysis as well. Furthermore, the development of open-source web platforms for programming DL models has expanded the frontiers of collaborative research in the development and validation of new

DL-based tools. A good example is provided by Ucuza et al., who developed web-based DL software aimed at the differential diagnosis of brain tumors using the popular Python programming language and the dedicated Keras library. Their software accepts multiple formats of the images, such as .jpeg, .jpg, and .png, and can be used to classify the input MRI image datasets into three diagnostic classes: meningioma, glioma, and pituitary tumors [36].

CNNs have a significant drawback in that they underutilize spatial relationships between the tumor and its surroundings, which is especially detrimental for classifying tumors. K. Adu and Y. Yu recently proposed a dilated capsule network model (CapsNet model), which is an extension of the traditional CNN, to address this issue [37]. In this model, the “routing by agreement” layer in the dilated CapsNet architecture takes the place of the pooling layer in the current CNN architecture [37]. Afshar et al. proposed a modified CapsNet architecture for classifying brain tumors that incorporates additional inputs into its pipeline from tissues surrounding the tumor, without detracting from the primary target, yielding satisfactory results [38].

Most AI-based classification algorithms target supratentorial tumors. In the posterior fossa, on the other hand, the two most common lesions in the adult population are hemangioblastoma, a benign tumor of vascular origin with a good survival rate, and brain metastases [39][40]. Obviously, discrimination between these entities is crucial for patient management as once again the therapeutic approach is different. In this field the role of AI-based is not yet well defined, however, a recent study attempted the differential diagnosis of intra-axial lesions of the posterior fossa using different radiomic algorithms (CNN, SVM, etc.), with promising results [1][41].

In some cases, even the differentiation between tumoral and non-tumoral processes is not simple. Tumefactive multiple sclerosis lesions, infection, inflammation disease (paraneoplastic syndrome and autoimmune disease), cortical dysplasia, and even stroke may be confused with tumoral processes, and accurate differential diagnosis based only on the radiological appearance is impossible due to the overlapping radiological features [42].

For example, tumefactive multiple sclerosis is a great mimicker of HGG on conventional MRI. The use of an AI-assisted tool can help the neuroradiologist to improve the differential diagnosis [4]: a recent study by Verma et al. achieved good results in differentiating GBMs from PCNSL from tumefactive multiple sclerosis lesions using an in-house software called dynamic texture parameter analysis (DTPA), which incorporates the analysis of quantitative texture parameters extracted from dynamic susceptibility contrast-enhanced (DSCE) sequences [43]. A more recent study by Han et al. evaluated the performance of different radiomic signature models in differentiating between low-grade glioma (LGG) and inflammation using radiomic features extracted from T1-weighted (T1WI) and T2-weighted (T2WI) MRI images. The features were chosen after a *t*-test and statistical regression (LASSO algorithm) to develop three radiomic models based on T1WI, T2WI, and combination (T1WI + T2WI), using, respectively four, eight, and five radiomic features each. The T2WI and combination models achieved better diagnostic efficacy in both the primary cohort and the validation cohort, significantly outperforming radiologist assessments [44].

## **4. Tumor Characterization**

In the era of molecular therapies, diagnostic neuroimaging should guide the diagnosis and treatment planning of brain tumors through a non-invasive characterization of the lesion, sometimes also called “virtual biopsy”, based on radiomic and radiogenomic approaches [11].

To date, most studies have challenged ML models to address very general classification tasks for brain tumors, such as differentiating between GBM and brain metastases [45][46]. However, more recently, researchers focused on the development of AI-driven tools, aiming to recognize the radiological signature of the tumor to provide a comprehensive analysis of the grading, genomic and epigenomic landscape of cerebral gliomas, which is extremely useful for decision-making towards a personalized medicine perspective. Therefore, several studies have been published in recent years where AI algorithms are challenged in increasingly specific classification tasks, such as differentiation within different subgroups of gliomas, for example, low-grade gliomas (LGGs) compared to high-grade gliomas (HGGs) [47][48]; isocitrate dehydrogenase (IDH) wild-type (IDH(-)) vs. IDH-mutated (IDH(+)) [49]; 1p/19q chromosomal arm deletion [50]; and others.

Several studies have focused on glioma grading. For example, Cho et al. used a radiomics approach to test the performance of various ML classifiers in determining the grading of 285 glioma cases (210 HGG, 75 LGG) obtained from the Brain Tumor Segmentation 2017 Challenge. The researchers extracted a large set of radiomic features from routine brain MRI sequences, including T1-weighted, T1-weighted contrast-enhanced, T2-weighted, and FLAIR. Three supervised ML classifiers showed an average AUC of 0.9400 for training cohorts and 0.9030 (logistic regression 0.9010, support vector machine 0.8866, and random forest 0.9213) for test cohorts [51].

In another study, Tian et al. investigated the role of radiomics in differentiating grade II gliomas from grade III and IV; they extracted radiomics features from conventional, diffusion, and perfusion arterial spin labeling (ASL) MRI. After multiparametric MRI preprocessing, high-throughput texture and histogram parameters features were derived from patients' volumes of interest (VOIs). Then, the support vector machine (SVM) classifier showed good accuracy/AUC (96.8%/0.987) for classifying LGGs from HGGs, and 98.1%/0.992, respectively, for classifying grades III from IV. Furthermore, they proved that texture features were more effective for non-invasively grading gliomas than histogram parameters [52].

Mzoughi et al. proposed a fully automatic deep multi-scale 3D CNN architecture for MRI gliomas brain tumor classification into low-grade gliomas and high-grade gliomas, using the whole volumetric T1 contrast-enhancement MRI sequence. For effective training, they used a data augmentation technique. After data augmentation and proper validation, the proposed approach achieved 96.49% accuracy, confirming that adequate MRI pre-processing and data augmentation could lead to the development of an accurate classification model when exploiting CNN-based approaches [53].

Chang et al. used CNNs for the differential diagnosis between IDH-mutant and IDH wild-type gliomas on conventional MRI imaging, achieving 92% accuracy; these results were in line with prior hypotheses based on visual assessment and underlying pathophysiology, as IDH wild-type lesions are characterized by more infiltrative and ill-defined borders. Furthermore, the authors found that nodular and heterogeneous contrast enhancement and "mass-like FLAIR edema" could aid in the prediction of MGMT methylation status, with up to 83% accuracy [54].

In another study, Kim et al. aimed to evaluate the added value of radiomic features extracted from MRI DWI and perfusion sequences in the prediction of IDH mutation and tumor grading in LGGs. For the IDH mutation, the model trained with multiparametric features showed similar performance to the model based on conventional sequences, but in tumor grading, it showed higher performance. This trend was confirmed in the independent validation set, demonstrating that DWI features and especially the apparent diffusion coefficient (ADC) map play a significant role in tumor grading [49].

In one of the first studies in the field, Akkus et al. presented a non-invasive method to predict 1p/19q chromosomal arm deletion from post-contrast T1- and T2-weighted MR images using a multi-scale CNN. They found that increased enhancement, infiltrative margins, and left frontal lobe predilection are associated with 1p19q codeletion with up to 93% accuracy [50].

In a larger, recent retrospective study, Meng et al. specifically targeted ATRX status in 123 patients diagnosed with gliomas (World Health Organization grades II–IV) using radiomics analysis, showing that radiomic features derived from preoperative MRI facilitate the efficient prediction of ATRX status in gliomas, achieving an AUC for ATRX mutation (ATRX(-)) of 0.84 (95% CI: 0.63–0.91) on the validation set, with a sensitivity, specificity, and accuracy of 0.73, 0.86, and 0.79, respectively [55].

In another retrospective study by Ren et al., researchers focused on the non-invasive prediction of molecular status for both IDH1 mutation and ATRX expression loss in LGGs, exploiting a radiomic approach based on high-throughput multiparametric MRI radiomic features. An optimal features subset was selected using a support vector machine (SVM) algorithm and ROC curve analysis was employed to assess the efficiency for the identification of the IDH1(+) and ATRX (-) status. Using 28 optimal texture features extracted from multiple MRI sequences, the SVM predictive model achieved excellent performances in terms of accuracies/AUCs/sensitivity/specificity/PPV/NPV in the prediction of IDH1(+) (94.74%/0.931/100%/85.71%/92.31%/100%, respectively) and ATRX (-) within LGGs (91.67%/0.926/94.74%/88.24%/90.00%/93.75%) [56].

Recently, some more ambitious studies have investigated the diagnostic accuracy of a radiomic approach in evaluating both the grading and the complete molecular profile of cerebral gliomas [57]. For instance, Habould et al. integrated clinical and laboratory data into a completely automated segmentation-based radiomics tool for the prediction of molecular status (ATRX, IDH1/2, MGMT, and 1p19q co-deletion), also distinguishing low-grade from high-grade gliomas. The system provided an AUC (validation/test) of  $0.981 \pm 0.015/0.885 \pm 0.02$  for the grading task. The prediction of the ATRX (-) condition had the best results, with an AUC of  $0.979 \pm 0.028/0.923 \pm 0.045$ , followed by the prediction of IDH1/2(+), with an AUC of  $0.929 \pm 0.042/0.861 \pm 0.023$ , while they showed only moderate results for the prediction of 1p19q and MGMT status [58].

In a similar study, Shboul et al. performed a non-invasive analysis of 108 pre-operative LGGs using imaging features to predict the status of MGMT methylation, IDH mutations, 1p/19q co-deletion, ATRX mutation, and TERT mutations, achieving a good accuracy with AUC of  $0.83 \pm 0.04$ ,  $0.84 \pm 0.03$ ,  $0.80 \pm 0.04$ ,  $0.70 \pm 0.09$ , and  $0.82 \pm 0.04$  [59].

A recent study focused on the detailed analysis of the tumor landscape within HGGs, highlighting the outstanding potential of DL algorithms in the extraction of new imaging markers, otherwise impossible to evaluate visually or with traditional radiomics approaches. Calabrese et al. retrospectively analyzed preoperative MRI data from 400 patients with WHO grade 4 glioblastoma or astrocytoma, who underwent resection and genetic testing to assess the status of nine key biomarkers: hotspot mutations of IDH1 or TERT promoter, pathogenic mutations of TP53, PTEN, ATRX, or CDKN2A/B, MGMT promoter methylation, EGFR amplification, and combined aneuploidy of chromosomes 7 and 10. An AI-driven model was tested in the prediction of biomarker status from MRI data using radiomics features, DL-based CNN features, and a combination of both. The results showed that the combination of radiomics and CNN features from preoperative MRI yields improved non-invasive genetic biomarker prediction performance in patients with WHO grade 4 diffuse astrocytic gliomas [60].

## References

1. Abdel Razek, A.A.K.; Alksas, A.; Shehata, M.; AbdelKhalek, A.; Abdel Baky, K.; El-Baz, A.; Helmy, E. Clinical Applications of Artificial Intelligence and Radiomics in Neuro-Oncology Imaging. *Insights Imaging* 2021, 12, 152.
2. Wesseling, P.; Capper, D. WHO 2016 Classification of Gliomas. *Neuropathol. Appl. Neurobiol.* 2018, 44, 139–150.
3. Jiang, H.; Cui, Y.; Wang, J.; Lin, S. Impact of Epidemiological Characteristics of Supratentorial Gliomas in Adults Brought about by the 2016 World Health Organization Classification of Tumors of the Central Nervous System. *Oncotarget* 2017, 8, 20354–20361.
4. Ceravolo, I.; Barchetti, G.; Biraschi, F.; Gerace, C.; Pampana, E.; Pingi, A.; Stasolla, A. Early Stage Glioblastoma: Retrospective Multicentric Analysis of Clinical and Radiological Features. *Radiol. Med.* 2021, 126, 1468–1476.
5. Louis, D.N.; Ohgaki, H.; Wiestler, O.D.; Cavenee, W.K.; Burger, P.C.; Jouvet, A.; Scheithauer, B.W.; Kleihues, P. The 2007 WHO Classification of Tumours of the Central Nervous System. *Acta Neuropathol.* 2007, 114, 97–109.
6. Louis, D.N.; Perry, A.; Reifenberger, G.; von Deimling, A.; Figarella-Branger, D.; Cavenee, W.K.; Ohgaki, H.; Wiestler, O.D.; Kleihues, P.; Ellison, D.W. The 2016 World Health Organization Classification of Tumors of the Central Nervous System: A Summary. *Acta Neuropathol.* 2016, 131, 803–820.
7. Capper, D.; Jones, D.T.W.; Sill, M.; Hovestadt, V.; Schrimpf, D.; Sturm, D.; Koelsche, C.; Sahm, F.; Chavez, L.; Reuss, D.E.; et al. DNA Methylation-Based Classification of Central Nervous System Tumours. *Nature* 2018, 555, 469–474.
8. Luger, A.-L.; König, S.; Samp, P.F.; Urban, H.; Divé, I.; Burger, M.C.; Voss, M.; Franz, K.; Fokas, E.; Filipiński, K.; et al. Molecular Matched Targeted Therapies for Primary Brain Tumors—A Single Center Retrospective Analysis. *J. Neurooncol.* 2022, 159, 243–259.
9. Di Bonaventura, R.; Montano, N.; Giordano, M.; Gessi, M.; Gaudino, S.; Izzo, A.; Mattogno, P.P.; Stumpo, V.; Caccavella, V.M.; Giordano, C.; et al. Reassessing the Role of Brain Tumor Biopsy in the Era of Advanced Surgical, Molecular, and Imaging Techniques—A Single-Center Experience with Long-Term Follow-Up. *J. Pers. Med.* 2021, 11, 909.
10. Singh, G.; Manjila, S.; Sakla, N.; True, A.; Wardeh, A.H.; Beig, N.; Vaysberg, A.; Matthews, J.; Prasanna, P.; Spektor, V. Radiomics and Radiogenomics in Gliomas: A Contemporary Update. *Br. J. Cancer* 2021, 125, 641–657.
11. Vagvala, S.; Guenette, J.P.; Jaimes, C.; Huang, R.Y. Imaging Diagnosis and Treatment Selection for Brain Tumors in the Era of Molecular Therapeutics. *Cancer Imaging* 2022, 22, 19.
12. Rudie, J.D.; Rauschecker, A.M.; Bryan, R.N.; Davatzikos, C.; Mohan, S. Emerging Applications of Artificial Intelligence in Neuro-Oncology. *Radiology* 2019, 290, 607–618.
13. Lambin, P.; Rios-Velazquez, E.; Leijenaar, R.; Carvalho, S.; van Stiphout, R.G.P.M.; Granton, P.; Zegers, C.M.L.; Gillies, R.; Boellard, R.; Dekker, A.; et al. Radiomics: Extracting More Information from Medical Images Using Advanced Feature Analysis. *Eur. J. Cancer* 2012, 48, 441–446.
14. Hosny, A.; Parmar, C.; Quackenbush, J.; Schwartz, L.H.; Aerts, H.J.W.L. Artificial Intelligence in Radiology. *Nat. Rev. Cancer* 2018, 18, 500–510.
15. Scapicchio, C.; Gabelloni, M.; Barucci, A.; Cioni, D.; Saba, L.; Neri, E. A Deep Look into Radiomics. *Radiol. Med.* 2021, 126, 1296–1311.
16. Mayerhoefer, M.E.; Materka, A.; Langs, G.; Häggström, I.; Szczypiński, P.; Gibbs, P.; Cook, G. Introduction to Radiomics. *J. Nucl. Med.* 2020, 61, 488–495.
17. Irmici, G.; Cè, M.; Caloro, E.; Khenkina, N.; Della Pepa, G.; Ascenti, V.; Martinenghi, C.; Papa, S.; Oliva, G.; Cellina, M. Chest X-Ray in Emergency Radiology: What Artificial Intelligence Applications Are Available? *Diagnostics* 2023, 13, 216.

18. Soda, P.; D'Amico, N.C.; Tessadori, J.; Valbusa, G.; Guarrasi, V.; Bortolotto, C.; Akbar, M.U.; Sicilia, R.; Cordelli, E.; Faz zini, D.; et al. AlforCOVID: Predicting the Clinical Outcomes in Patients with COVID-19 Applying AI to Chest-X-Rays. An Italian Multicentre Study. *Med. Image Anal.* 2021, 74, 102216.
19. Pope, W.B. Brain Metastases: Neuroimaging. *Handb. Clin. Neurol.* 2018, 149, 89–112.
20. Cellina, M.; Cè, M.; Irmici, G.; Ascenti, V.; Khenkina, N.; Toto-Brocchi, M.; Martinenghi, C.; Papa, S.; Carrafiello, G. Artificial Intelligence in Lung Cancer Imaging: Unfolding the Future. *Diagnostics* 2022, 12, 2644.
21. Park, J.E. Artificial Intelligence in Neuro-Oncologic Imaging: A Brief Review for Clinical Use Cases and Future Perspectives. *Brain Tumor Res. Treat.* 2022, 10, 69.
22. Park, Y.W.; Jun, Y.; Lee, Y.; Han, K.; An, C.; Ahn, S.S.; Hwang, D.; Lee, S.-K. Robust Performance of Deep Learning for Automatic Detection and Segmentation of Brain Metastases Using Three-Dimensional Black-Blood and Three-Dimensional Gradient Echo Imaging. *Eur. Radiol.* 2021, 31, 6686–6695.
23. Voicu, I.P.; Pravata, E.; Panara, V.; Navarra, R.; Mattei, P.A.; Caulo, M. Differentiating Solitary Brain Metastases from High-Grade Gliomas with MR: Comparing Qualitative versus Quantitative Diagnostic Strategies. *Radiol. Med.* 2022, 127, 891–898.
24. Bauer, A.H.; Erly, W.; Moser, F.G.; Maya, M.; Nael, K. Differentiation of Solitary Brain Metastasis from Glioblastoma Multiforme: A Predictive Multiparametric Approach Using Combined MR Diffusion and Perfusion. *Neuroradiology* 2015, 57, 697–703.
25. Romano, A.; Moltoni, G.; Guarnera, A.; Pasquini, L.; Di Napoli, A.; Napolitano, A.; Espagnet, M.C.R.; Bozzao, A. Single Brain Metastasis versus Glioblastoma Multiforme: A VOI-Based Multiparametric Analysis for Differential Diagnosis. *Radiol. Med.* 2022, 127, 490–497.
26. Swinburne, N.C.; Schefflein, J.; Sakai, Y.; Oermann, E.K.; Titano, J.J.; Chen, I.; Tadayon, S.; Aggarwal, A.; Doshi, A.; Nael, K. Machine Learning for Semi-automated Classification of Glioblastoma, Brain Metastasis and Central Nervous System Lymphoma Using Magnetic Resonance Advanced Imaging. *Ann. Transl. Med.* 2019, 7, 232.
27. Upadhyay, N.; Waldman, A.D. Conventional MRI Evaluation of Gliomas. *Br. J. Radiol.* 2011, 84, S107–S111.
28. Skogen, K.; Schulz, A.; Helseth, E.; Ganeshan, B.; Dormagen, J.B.; Server, A. Texture Analysis on Diffusion Tensor Imaging: Discriminating Glioblastoma from Single Brain Metastasis. *Acta Radiol.* 2019, 60, 356–366.
29. Han, Y.; Zhang, L.; Niu, S.; Chen, S.; Yang, B.; Chen, H.; Zheng, F.; Zang, Y.; Zhang, H.; Xin, Y.; et al. Differentiation between Glioblastoma Multiforme and Metastasis from the Lungs and Other Sites Using Combined Clinical/Routine MRI Radiomics. *Front. Cell Dev. Biol.* 2021, 9, 710461.
30. Nayak, L.; Lee, E.Q.; Wen, P.Y. Epidemiology of Brain Metastases. *Curr. Oncol. Rep.* 2012, 14, 48–54.
31. Ortiz-Ramón, R.; Larroza, A.; Ruiz-España, S.; Arana, E.; Moratal, D. Classifying Brain Metastases by Their Primary Site of Origin Using a Radiomics Approach Based on Texture Analysis: A Feasibility Study. *Eur. Radiol.* 2018, 28, 4514–4523.
32. Barajas, R.F.; Politi, L.S.; Anzalone, N.; Schöder, H.; Fox, C.P.; Boxerman, J.L.; Kaufmann, T.J.; Quarles, C.C.; Ellingson, B.M.; Auer, D.; et al. Consensus Recommendations for MRI and PET Imaging of Primary Central Nervous System Lymphoma: Guideline Statement from the International Primary CNS Lymphoma Collaborative Group (IPCG). *Neuro Oncol.* 2021, 23, 1056–1071.
33. Tang, Y.Z.; Booth, T.C.; Bhogal, P.; Malhotra, A.; Wilhelm, T. Imaging of Primary Central Nervous System Lymphoma. *Clin. Radiol.* 2011, 66, 768–777.
34. Cai, Q.; Fang, Y.; Young, K.H. Primary Central Nervous System Lymphoma: Molecular Pathogenesis and Advances in Treatment. *Transl. Oncol.* 2019, 12, 523–538.
35. Stadlbauer, A.; Marhold, F.; Oberndorfer, S.; Heinz, G.; Buchfelder, M.; Kinfe, T.M.; Meyer-Bäse, A. Radiophysiomics: Brain Tumors Classification by Machine Learning and Physiological MRI Data. *Cancers* 2022, 14, 2363.
36. Ucuzal, H.; Yasar, S.; Colak, C. Classification of Brain Tumor Types by Deep Learning with Convolutional Neural Network on Magnetic Resonance Images Using a Developed Web-Based Interface. In Proceedings of the 2019 3rd International Symposium on Multidisciplinary Studies and Innovative Technologies (ISMSIT), Ankara, Turkey, 11–13 October 2019; IEEE: Piscataway, NJ, USA, 2019; pp. 1–5.
37. Adu, K.; Yu, Y.; Cai, J.; Tashi, N. Dilated Capsule Network for Brain Tumor Type Classification via MRI Segmented Tumor Region. In Proceedings of the 2019 IEEE International Conference on Robotics and Biomimetics (ROBIO), Dali, China, 6–8 December 2019; IEEE: Piscataway, NJ, USA, 2019; pp. 942–947.
38. Afshar, P.; Plataniotis, K.N.; Mohammadi, A. Capsule Networks for Brain Tumor Classification Based on MRI Images and Coarse Tumor Boundaries. In Proceedings of the ICASSP 2019–2019 IEEE International Conference on Acoustics, S

39. Sunderland, G.J.; Jenkinson, M.D.; Zakaria, R. Surgical Management of Posterior Fossa Metastases. *J. Neurooncol.* **2016**, *130*, 535–542.
40. She, D.; Yang, X.; Xing, Z.; Cao, D. Differentiating Hemangioblastomas from Brain Metastases Using Diffusion-Weighted Imaging and Dynamic Susceptibility Contrast-Enhanced Perfusion-Weighted MR Imaging. *Am. J. Neuroradiol.* **2016**, *37*, 1844–1850.
41. Payabvash, S.; Aboian, M.; Tihan, T.; Cha, S. Machine Learning Decision Tree Models for Differentiation of Posterior Fossa Tumors Using Diffusion Histogram Analysis and Structural MRI Findings. *Front. Oncol.* **2020**, *10*, 71.
42. Lin, X.; Yu, W.-Y.; Liao, L.; Chander, R.J.; Soon, W.E.; Lee, H.Y.; Tan, K. Clinicoradiologic Features Distinguish Tumefactive Multiple Sclerosis from CNS Neoplasms. *Neurol. Clin. Pract.* **2017**, *7*, 53–64.
43. Verma, R.K.; Wiest, R.; Locher, C.; Heldner, M.R.; Schucht, P.; Raabe, A.; Gralla, J.; Kamm, C.P.; Slotboom, J.; Kellner, W.; Weldon, F. Differentiating Enhancing Multiple Sclerosis Lesions, Glioblastoma, and Lymphoma with Dynamic Texture Parameters Analysis: A Feasibility Study. *Med. Phys.* **2017**, *44*, 4000–4008.
44. Han, Y.; Yang, Y.; Shi, Z.; Zhang, A.; Yan, L.; Hu, Y.; Feng, L.; Ma, J.; Wang, W.; Cui, G. Distinguishing Brain Inflammation from Grade II Glioma in Population without Contrast Enhancement: A Radiomics Analysis Based on Conventional MRI. *Eur. J. Radiol.* **2021**, *134*, 109467.
45. Qian, Z.; Li, Y.; Wang, Y.; Li, L.; Li, R.; Wang, K.; Li, S.; Tang, K.; Zhang, C.; Fan, X.; et al. Differentiation of Glioblastoma from Solitary Brain Metastases Using Radiomic Machine-Learning Classifiers. *Cancer Lett.* **2019**, *451*, 128–135.
46. Bae, S.; An, C.; Ahn, S.S.; Kim, H.; Han, K.; Kim, S.W.; Park, J.E.; Kim, H.S.; Lee, S.-K. Robust Performance of Deep Learning for Distinguishing Glioblastoma from Single Brain Metastasis Using Radiomic Features: Model Development and Validation. *Sci. Rep.* **2020**, *10*, 12110.
47. Wiestler, B.; Kluge, A.; Lukas, M.; Gempt, J.; Ringel, F.; Schlegel, J.; Meyer, B.; Zimmer, C.; Förster, S.; Pyka, T.; et al. Multiparametric MRI-Based Differentiation of WHO Grade II/III Glioma and WHO Grade IV Glioblastoma. *Sci. Rep.* **2016**, *6*, 35142.
48. Zhang, X.; Yan, L.-F.; Hu, Y.-C.; Li, G.; Yang, Y.; Han, Y.; Sun, Y.-Z.; Liu, Z.-C.; Tian, Q.; Han, Z.-Y.; et al. Optimizing a Machine Learning Based Glioma Grading System Using Multi-Parametric MRI Histogram and Texture Features. *Oncotarget* **2017**, *8*, 47816–47830.
49. Kim, M.; Jung, S.Y.; Park, J.E.; Jo, Y.; Park, S.Y.; Nam, S.J.; Kim, J.H.; Kim, H.S. Diffusion- and Perfusion-Weighted MRI Radiomics Model May Predict Isocitrate Dehydrogenase (IDH) Mutation and Tumor Aggressiveness in Diffuse Lower Grade Glioma. *Eur. Radiol.* **2020**, *30*, 2142–2151.
50. Akkus, Z.; Ali, I.; Sedlář, J.; Agrawal, J.P.; Parney, I.F.; Giannini, C.; Erickson, B.J. Predicting Deletion of Chromosomal Arms 1p/19q in Low-Grade Gliomas from MR Images Using Machine Intelligence. *J. Digit. Imaging* **2017**, *30*, 469–476.
51. Cho, H.; Lee, S.; Kim, J.; Park, H. Classification of the Glioma Grading Using Radiomics Analysis. *PeerJ* **2018**, *6*, e5982.
52. Tian, Q.; Yan, L.-F.; Zhang, X.; Zhang, X.; Hu, Y.-C.; Han, Y.; Liu, Z.-C.; Nan, H.-Y.; Sun, Q.; Sun, Y.-Z.; et al. Radiomics Strategy for Glioma Grading Using Texture Features from Multiparametric MRI. *J. Magn. Reson. Imaging* **2018**, *48*, 1518–1528.
53. Mzoughi, H.; Njeh, I.; Wali, A.; Slima, M.B.; BenHamida, A.; Mhiri, C.; Mahfoudhe, K.B. Deep Multi-Scale 3D Convolutional Neural Network (CNN) for MRI Gliomas Brain Tumor Classification. *J. Digit. Imaging* **2020**, *33*, 903–915.
54. Chang, P.; Grinband, J.; Weinberg, B.D.; Bardis, M.; Khy, M.; Cadena, G.; Su, M.-Y.; Cha, S.; Filippi, C.G.; Bota, D.; et al. Deep-Learning Convolutional Neural Networks Accurately Classify Genetic Mutations in Gliomas. *Am. J. Neuroradiol.* **2018**, *39*, 1201–1207.
55. Meng, L.; Zhang, R.; Fa, L.; Zhang, L.; Wang, L.; Shao, G. ATRX Status in Patients with Gliomas: Radiomics Analysis. *Medicine* **2022**, *101*, e30189.
56. Ren, Y.; Zhang, X.; Rui, W.; Pang, H.; Qiu, T.; Wang, J.; Xie, Q.; Jin, T.; Zhang, H.; Chen, H.; et al. Noninvasive Prediction of IDH1 Mutation and ATRX Expression Loss in Low-Grade Gliomas Using Multiparametric MR Radiomic Features. *J. Magn. Reson. Imaging* **2019**, *49*, 808–817.
57. Alentorn, A.; Duran-Peña, A.; Pingle, S.C.; Piccioni, D.E.; Idbaih, A.; Kesari, S. Molecular profiling of gliomas: Potential therapeutic implications. *Expert Rev. Anticancer Ther.* **2015**, *15*, 955–962.
58. Haubold, J.; Hosch, R.; Parmar, V.; Glas, M.; Guberina, N.; Catalano, O.A.; Pierscianek, D.; Wrede, K.; Deuschl, C.; Forsting, M.; et al. Fully Automated MR Based Virtual Biopsy of Cerebral Gliomas. *Cancers* **2021**, *13*, 6186.



59. Shboul, Z.A.; Chen, J.; Iftekharuddin, K.M. Prediction of Molecular Mutations in Diffuse Low-Grade Gliomas Using MR I  
maging Features. *Sci. Rep.* 2020, 10, 3711.
60. Calabrese, E.; Rudie, J.D.; Rauschecker, A.M.; Villanueva-Meyer, J.E.; Clarke, J.L.; Solomon, D.A.; Cha, S. Combining  
Radiomics and Deep Convolutional Neural Network Features from Preoperative MRI for Predicting Clinically Relevant  
Genetic Biomarkers in Glioblastoma. *Neuro-Oncol. Adv.* 2022, 4, vdac060.

---

Retrieved from <https://encyclopedia.pub/entry/history/show/95552>